

Table of contents

Sections	Titles	Pages
Section S1	Experimental section (Instrumentations and Computational Descriptions).	S3-4
Table S1	Crystal data and structure refinement for RbSbF ₃ Cl and Rb ₃ Sb ₄ F ₁₄ Cl.	S5
Table S2	Atomic coordinates and equivalent isotropic displacement parameters for RbSbF ₃ Cl.	S6
Table S3	Atomic coordinates and equivalent isotropic displacement parameters for Rb ₃ Sb ₄ F ₁₄ Cl.	S7
Table S4	Selected bond lengths (Å) and angles [°] for RbSbF ₃ Cl.	S8
Table S5	Selected bond lengths (Å) and angles [°] for Rb ₃ Sb ₄ F ₁₄ Cl.	S9
Table S6	The density of Sb ³⁺ cations in a unit cell.	S10
Table S7	LDT test results of AgGaS ₂ , RbSbF ₃ Cl, and Rb ₃ Sb ₄ F ₁₄ Cl.	S11
Table S8	Calculation of dipole moment for [SbF ₃ Cl ₂] ²⁻ polyhedra and net dipole moment for a unit cell in RbSbF ₃ Cl (D = Debyes).	S12
Table S9	Calculation of dipole moment for [SbF ₃ Cl ₂] ²⁻ , [SbF ₅] ²⁻ , and [SbF ₄] ⁻ polyhedra and net dipole moment for a unit cell in Rb ₃ Sb ₄ F ₁₄ Cl (D = Debyes).	S13
Fig. S1	The crystal photographs of (a) RbSbF ₃ Cl and (b) Rb ₃ Sb ₄ F ₁₄ Cl.	S14
Fig. S2	The coordination modes of Rb ⁺ cations in (a) RbSbF ₃ Cl and (b) Rb ₃ Sb ₄ F ₁₄ Cl.	S14
Fig. S3	Powder X-ray diffraction patterns of (a) RbSbF ₃ Cl and (b) Rb ₃ Sb ₄ F ₁₄ Cl.	S15
Fig. S4	TGA curves of (a) RbSbF ₃ Cl and (b) Rb ₃ Sb ₄ F ₁₄ Cl.	S15
Fig. S5	UV-vis-NIR optical diffuse reflectance spectra of (a) RbSbF ₃ Cl and (b) Rb ₃ Sb ₄ F ₁₄ Cl.	S16
Fig. S6	Calculated refractive index for RbSbF ₃ Cl.	S16
References		S17

Section S1. Experimental section

Instrumentations.

The single-crystal data for RbSbF_3Cl and $\text{Rb}_3\text{Sb}_4\text{F}_{14}\text{Cl}$ were collected using a Rigaku XtaLAB Synergy R diffractometer and analyzed with SHELX-2014.¹ The coordinates of each atom were refined using a least squares plane convergence algorithm based on the F^2 full matrix. The space group was further analyzed with PLATON, confirming no higher symmetry group.² Crystallographic data and additional relevant details for the compound are summarized in Tables S1–S5.

The powder X-ray diffraction data were collected at room temperature using a SmartLab diffractometer with $\text{Cu K}\alpha$ radiation ($\lambda = 1.540598 \text{ \AA}$). The data were acquired over a 2θ range of 5° – 70° at a scanning rate of 8° min^{-1} with a step width of 0.02° .

Thermogravimetric analysis (TGA) measurements were tested using Discovery-TGA thermal analyzer. The sample was heated from room temperature to 750°C under a nitrogen atmosphere, and the heating rate was set to be $10^\circ\text{C}\cdot\text{min}^{-1}$.

The infrared spectra of two compounds were recorded at room temperature using a Vertex 70 Fourier-transform infrared spectrometer (FTIR) within the 400 – 4000 cm^{-1} range. The sample, in powdered form, was mixed with KBr at a 1:100 ratio and pressed into a transparent pellet for analysis.

The UV–vis–NIR diffuse reflectance spectra were measured using a Shimadzu UV-2600 spectrophotometer, covering a wavelength range from 200 – 2500 nm .

The birefringence of RbSbF_3Cl was measured using a polarizing microscope (Carl Zeiss Axioscope 5) with the light source wavelength of 546 nm .

The LDT of two crystals were measured with a Nd:YAG laser of 1064 nm wavelength and 10 ns pulse width. For comparison, the LDT of AgGaS_2 (AGS), which is available commercially, was also measured in the same scenario.

The SHG efficiency of both the compounds was determined following the Kurtz and Perry method,³ utilizing a Q-switched Nd:YAG laser at 1064 nm . To investigate the effect of particle size on SHG efficiency, the crystal was ground into the following

size ranges: 25–45, 45–58, 58–75, 75–106, 106–150, and 150–212 μm . The reference material KH_2PO_4 (KDP) was also measured with the same size.

Computational Descriptions.

To understand the electronic structure of RbSbF_3Cl and $\text{Rb}_3\text{Sb}_4\text{F}_{14}\text{Cl}$, density functional theory (DFT) calculations were performed to determine the band structure, density of states (DOS), and partial density of states (PDOS).⁴ The calculations employed the Perdew-Burke-Ernzerhof (PBE)⁵ functional within the generalized gradient approximation (GGA), using norm-conserving pseudopotentials.⁶ The criteria of convergences of energy was set as 1.0×10^{-6} eV/atom, and the criteria of convergence of force was set as 0.03 eV/Å. The kinetic energy cutoff of them was 850 eV, and their k-point sampling dimensions in Brillouin were $3 \times 3 \times 4$ and $1 \times 2 \times 2$, respectively.

Table S1. Crystal data and structure refinement for RbSbF₃Cl and Rb₃Sb₄F₁₄Cl.

Formula	RbSbF ₃ Cl	Rb ₃ Sb ₄ F ₁₄ Cl
Formula weight	300.28	1044.86
Crystal System	tetragonal	orthorhombic
Space Group	$\bar{I}42m$	$Pmn2_1$
<i>a</i> (Å)	9.8659 (2)	30.5126 (9)
<i>b</i> (Å)	9.8659 (2)	7.4783 (2)
<i>c</i> (Å)	10.8193 (4)	7.3322 (2)
<i>α</i> (°)	90	90
<i>β</i> (°)	90	90
<i>γ</i> (°)	90	90
<i>V</i> (Å ³)	1053.11 (6)	1673.08(8)
<i>Z</i>	8	4
ρ (calcd) (g/cm ³)	3.788	4.148
Temperature (K)	297.28 (10)	298.63(10)
<i>F</i> (000)	1058.0	1832.0
μ (mm ⁻¹)	14.878	15.344
<i>R</i> ₁ , <i>wR</i> ₂ (<i>I</i> > 2σ(<i>I</i>)) ^a	0.0160/0.0367	0.0203/0.0374
GOF on <i>F</i> ²	1.078	1.024

$$^a R_1(F) = \sum ||F_o| - |F_c|| / \sum |F_o|. \quad wR_2(F_o^2) = [\sum w(F_o^2 - F_c^2)^2 / \sum w(F_o^2)^2]^{1/2}$$

Table S2. Atomic coordinates ($\times 10^4$) and equivalent isotropic displacement parameters ($\text{\AA}^2 \times 10^3$) for RbSbF_3Cl . $U_{(\text{eq})}$ is defined as one third of the trace of the orthogonalized U_{ij} tensor.

atom	x	y	z	$U_{\text{eq}}(\text{\AA}^2)$	BVS
Sb1	2886.9 (4)	7113.1 (4)	5446.4 (5)	21.78 (14)	3.11
Rb1	5000	5000	8032.7 (8)	33.0 (2)	0.98
Rb2	5000	10000	7500	38.1 (2)	1.00
Cl1	2872 (2)	10000	5000	43.3 (4)	0.89
F1	4644 (3)	7295 (4)	6280 (3)	49.4 (8)	1.05
F2	2186 (4)	7814 (4)	6970 (4)	61.8 (13)	1.29

Table S3. Atomic coordinates ($\times 10^4$) and equivalent isotropic displacement parameters ($\text{\AA}^2 \times 10^3$) for $\text{Rb}_3\text{Sb}_4\text{F}_{14}\text{Cl}$. $U_{(\text{eq})}$ is defined as one third of the trace of the orthogonalized U_{ij} tensor.

atom	x	y	z	$U_{\text{eq}} (\text{\AA}^2)$	BVS
Sb1	5000	10689.2 (5)	7153.7 (7)	19.48 (13)	3.08
Sb2	5000	4115.4 (6)	2591.4 (8)	24.05 (13)	3.20
Sb3	4239.0 (2)	8638.9 (4)	2324.3 (6)	20.17 (8)	3.00
Sb4	3531.4 (2)	10568.7 (4)	6768.8 (5)	21.98 (9)	2.90
Sb5	2795.2 (2)	5544.8 (4)	6914.2 (5)	20.15 (9)	3.09
Rb1	4246.7 (2)	5854.8 (7)	7346.7 (11)	39.19 (16)	0.93
Rb2	3551.9 (2)	13968.0 (7)	2188.0 (9)	31.95 (14)	0.98
Rb3	2105.1 (2)	897.9 (6)	6719.8 (10)	28.45 (15)	1.15
Cl1	5718.6 (5)	11862.9 (19)	9434 (2)	35.2 (3)	1.09
F1	5000	8711 (6)	8836 (7)	44.8 (13)	1.02
F2	4553.5 (10)	9297 (4)	5849 (5)	38.0 (8)	0.96
F3	5450.1 (15)	3161 (6)	4255 (7)	80.0 (15)	0.92
F4	5000	6069 (8)	4295 (8)	54.4 (15)	1.06
F5	4467.1 (10)	6027 (4)	1373 (5)	40.9 (8)	0.91
F6	3938.5 (10)	7060 (4)	3997 (5)	33.1 (7)	1.23
F7	3765.8 (9)	10335 (4)	3205 (5)	32.5 (7)	0.95
F8	3810.0 (10)	8008 (4)	500 (5)	36.6 (8)	1.09
F9	3592.9 (10)	13110 (4)	6105 (5)	36.9 (8)	1.05
F10	2994.1 (10)	10670 (5)	5399 (5)	41.1 (9)	1.19
F11	3194.6 (11)	11364 (5)	8851 (5)	42.4 (9)	1.11
F12	3222.8 (11)	7637 (5)	7523 (6)	59.0 (11)	0.90
F13	2920.2 (10)	6287 (5)	4427 (5)	39.6 (8)	1.11
F14	2365.8 (9)	7376 (3)	7264 (6)	38.3 (8)	1.26
F15	2268.2 (11)	4372 (4)	5602 (5)	37.8 (8)	0.92

Table S4. Selected bond distances (Å) and angles [°] for RbSbF₃Cl.

Sb1—F2	1.917 (4)	Cl1 ¹¹ —Rb2—Cl1	75.63 (5)
Sb1—F1	1.962 (3)	Cl1 ¹ —Rb2—Cl1 ¹¹	128.62 (3)
Sb1—Cl1 ³	2.8888 (4)	Cl1—Rb2—F2	52.76 (8)
Rb1—Cl1 ⁵	3.5441 (17)	Cl1 ¹ —Rb2—F2	119.89 (7)
Rb1—F1	2.974 (4)	F1 ¹ —Rb2—Cl1 ¹	65.19 (6)
Rb1—F2 ⁵	3.050 (5)	F1 ⁵ —Rb2—Cl1	153.33 (7)
Rb2—Cl1 ¹¹	3.4238 (13)	F1 ⁵ —Rb2—F1	101.17 (5)
Rb2—F1 ¹¹	2.998 (4)	F1 ⁵ —Rb2—F1 ¹	127.76 (12)
Rb2—F2	3.5620 (11)	F1—Rb2—F2 ¹	45.48 (10)
Cl1 ³ —Sb1—Cl1	87.84 (8)	F1—Rb2—F2 ¹	133.93 (10)
F1—Sb1—Cl1	89.50 (11)	F2 ¹¹ —Rb2—F2 ¹	91.49 (2)
F1—Sb1—Cl1 ³	161.32 (10)	F2 ¹ —Rb2—F2 ⁵	161.47 (14)
F2—Sb1—Cl1	77.65 (12)	Sb1 ¹² —Cl1—Rb1 ¹³	84.47 (3)
F2—Sb1—F1	83.72 (15)	Sb1—Cl1—Rb1 ¹³	95.99 (4)
F1 ⁴ —Sb1—F1	87.1 (2)	Sb1 ¹² —Cl1—Rb2 ¹⁴	82.24 (2)
Cl1 ⁷ —Rb1—Cl1 ⁶	68.86 (2)	Sb1—Cl1—Rb2 ¹⁴	97.41 (3)
Cl1 ⁵ —Rb1—Cl1 ⁶	106.18 (5)	Rb1 ¹³ —Cl1—Rb1 ¹	73.82 (5)
F1—Rb1—Cl1 ⁵	76.96 (7)	Rb2—Cl1—Rb1 ¹	90.904 (14)
F1 ⁴ —Rb1—Cl1 ⁷	172.57 (6)	Rb2 ¹⁴ —Cl1—Rb1 ¹	164.72 (5)
F1—Rb1—F1 ⁴	54.09 (11)	Rb2—Cl1—Rb2 ¹⁴	104.37 (5)
F1 ⁴ —Rb1—F1 ¹⁰	100.77 (13)	Sb1—F1—Rb1	109.15 (13)
F1 ⁴ —Rb1—F2 ⁶	62.92 (8)	Sb1—F1—Rb2	112.77 (15)
F1 ¹⁰ —Rb1—F2 ⁶	117.01 (8)	Rb1—F1—Rb2	112.52 (10)
F2 ⁶ —Rb1—Cl1 ⁶	55.61 (6)	Sb1—F2—Rb1 ¹	120.6 (2)
F2 ⁶ —Rb1—Cl1 ⁷	124.47 (7)	Sb1—F2—Rb2 ²	94.34 (8)
F2 ⁵ —Rb1—F2 ⁶	179.89 (18)	Rb1 ¹ —F2—Rb2 ²	97.08 (8)

Symmetry codes: (1)-1/2+y,3/2-x,3/2-z; (2)1/2-x,-1/2+y,3/2-z; (3)-1+y,1-x,1-z; (4)1-y,1-x,+z; (5)1/2+x,-1/2+y,1/2+z; (6)3/2-y,1/2+x,3/2-z; (7)-1/2+y,1/2-x,3/2-z; (8)1/2-x,3/2-y,1/2+z; (9)1-x,1-y,+z; (10)+y,+x,+z; (11)1-x,2-y,+z; (12)1-y,1+x,1-z; (13)-1/2+x,1/2+y,-1/2+z; (14)1-x,+y,1-z; (15)+y,1-x,1-z.

Table S5. Selected bond distances (Å) and angles [°] for Rb₃Sb₄F₁₄Cl.

Sb1—Cl1	2.8936 (15)	F1—Sb1—F2	84.54 (16)
Sb1—F1	1.926 (5)	F2 ⁴ —Sb1—F2	87.87 (19)
Sb1—F2	1.963 (3)	F4—Sb2—F5	77.52 (16)
Sb2—F4	1.923 (5)	F3 ⁴ —Sb2—F5 ⁴	160.21 (17)
Sb2—F5	2.342 (3)	F8—Sb3—F5	77.09 (13)
Sb3—F8	1.930 (3)	F7—Sb3—F5	152.46 (12)
Sb3—F5	2.188 (3)	F10—Sb4—F12	79.96 (13)
Sb4—F10	1.924 (3)	F9—Sb4—F12	162.85 (12)
Sb4—F12	2.450 (3)	F14—Sb5—F15	80.41 (13)
Sb5—F14	1.913 (2)	F15—Sb5—F12	154.66 (14)
Sb5—F12	2.085 (3)	Cl1 ¹² —Rb1—F12	111.12 (7)
Rb1—Cl1 ¹¹	3.3563 (16)	F3 ⁴ —Rb1—F4	47.54 (11)
Rb1—F6	2.780 (3)	F8 ¹¹ —Rb1—F3 ⁴	169.53 (10)
Rb1—F12	3.399 (4)	Cl1 ⁸ —Rb2—F3 ⁹	66.54 (8)
Rb2—Cl1 ⁸	3.3928 (16)	F5 ⁶ —Rb2—F8 ⁶	45.85 (7)
Rb2—F7	2.892 (3)	F14 ¹⁰ —Rb2—F5 ⁶	166.84 (9)
Rb2—F3 ¹⁰	3.454 (5)	F8 ⁵ —Rb3—F12 ¹	51.71 (8)
Rb3—F15	2.769 (3)	F10 ³ —Rb3—F7 ⁵	158.66 (9)
Rb3—F12 ¹	3.416 (4)	Sb1—Cl1—Rb2 ¹³	169.04 (5)
Cl1—Sb1—Cl1 ⁴	98.54 (6)	Sb1—F1—Rb1 ⁴	106.45 (16)
F1—Sb1—Cl1 ⁴	82.12 (11)	Sb1—F2—Rb1	120.08 (16)
F2 ⁴ —Sb1—Cl1 ⁴	165.50 (10)	Sb2—F3—Rb1 ⁴	114.57 (18)

Symmetry codes: (1) 1/2-x, 1-y, -1/2+z; (2) +x, +y, -1+z; (3) +x, -1+y, +z; (4) 1-x, +y, +z; (5) 1/2-x, 1-y, 1/2+z; (6)+x, 1+y, +z; (7) 1/2-x, 2-y, 1/2+z; (8) 1-x, +y, -1+z; (9) 1-x, 1+y, +z; (10) 1/2-x, 2-y, -1/2+z; (11) +x, +y, 1+z; (12) 1-x, -1+y, +z; (13) 1-x, +y, 1+z.

Table S6. The density of Sb^{3+} cations in a unit cell.

Compounds	n (Sb)	V (\AA^3)	ρ (Sb) (\AA^{-3})
RbSbF ₃ Cl	8	1053.11	0.0076
Rb ₃ Sb ₄ F ₁₄ Cl	18	1673.08	0.0110

n : the number of Sb^{3+} cations in a unit cell. V : the cell volume. ρ : the density of Sb^{3+} cations in a unit cell, $\rho=n/V$.

Table S7. LDT test results of AgGaS₂, RbSbF₃Cl, and Rb₃Sb₄F₁₄Cl.

Formula	Energy/mJ	Spot area/mm ²	Pulse width/ns	LDT/(MW/cm ²)
AgGaS ₂	3.0	20	10	30
RbSbF ₃ Cl	16.3	20	10	163
Rb ₃ Sb ₄ F ₁₄ Cl	22.3	20	10	223

Table S8. Calculation of dipole moment for $[\text{SbF}_3\text{Cl}_2]^{2-}$ polyhedra and net dipole moment for a unit cell in RbSbF_3Cl (D = Debyes).

RbSbF ₃ Cl				
Polar unit (aunit cell)	Dipole moment (D)			
	x-component	y-component	z-component	total magnitude
SbF ₃ Cl ₂	-8.501490841	8.501490841	-15.96604147	19.98662486
	8.501490841	-8.501490841	-15.96604147	19.98662486
	-8.501490841	-8.501490841	15.96604147	19.98662486
	8.501490841	8.501490841	15.96604147	19.98662486
	8.501490841	8.501490841	15.96604147	19.98662486
	-8.501490841	-8.501490841	15.96604147	19.98662486
	8.501490841	-8.501490841	-15.96604147	19.98662486
	-8.501490841	8.501490841	-15.96604147	19.98662486
	U_x	U_y	U_z	U_t
Net dipole moment	-1.95399E-14	-2.13163E-14	3.55271E-14	4.5808E-14
Cell Volume	1053.11 (6) Å ³			

Table S9. Calculation of dipole moment for $[\text{SbF}_3\text{Cl}_2]^{2-}$, $[\text{SbF}_5]^{2-}$ and $[\text{SbF}_4]^-$ polyhedra and net dipole moment for a unit cell in $\text{Rb}_3\text{Sb}_4\text{F}_{14}\text{Cl}$ (D = Debyes).

Rb ₃ Sb ₄ F ₁₄ Cl				
Polar unit (aunit cell)	Dipole moment (D)			
	x-component	y-component	z-component	total magnitude
Sb1F ₃ Cl ₂	0.000409587	-12.73467075	-11.72701802	17.3116952
	-0.000409587	-12.73467075	-11.72701802	17.3116952
	1.42109E-14	12.73415092	-11.73013085	17.31342165
	U_x	U_y	U_z	U_t
	2.66454E-15	-12.73519057	-35.18416688	37.41805284
Sb2F ₅	0	-10.99913869	-15.21747426	18.77638343
	-0.002023019	10.9992254	-15.20926125	18.76977867
	0.002023019	10.9992254	-15.20926125	18.76977867
	U_x	U_y	U_z	U_t
	6.21725E-15	10.99931212	-45.63599675	46.94282764
Sb3F ₄	17.63613625	11.22280952	0.248184832	20.90565357
	-17.63613625	11.22280952	0.248184832	20.90565357
	-17.63613625	-11.22280952	0.248184832	20.90565357
	17.63613625	-11.22280952	0.248184832	20.90565357
Sb4F ₄	-17.48122509	7.674077512	-1.933583367	19.18914904
	17.48122509	7.674077512	-1.933583367	19.18914904
	17.48110396	-7.674069815	-1.933572829	19.18903456
	-17.48110396	-7.674069815	-1.933572829	19.18903456
Sb5F ₄	-7.453914661	14.83178556	11.6110415	20.25731945
	7.458651183	-14.83381875	11.6135617	20.26199575
	-7.458701096	-14.83395227	11.61356981	20.26211651
	7.453914661	14.83178556	11.6110415	20.25731945
	U_x	U_y	U_z	U_t
	-0.000049913	-0.004184512	39.70764145	39.70764167
Net dipole moment	-0.000049913	-1.740062966	-41.11252218	41.14932927
Cell Volume	1673.08 (8) Å ³			

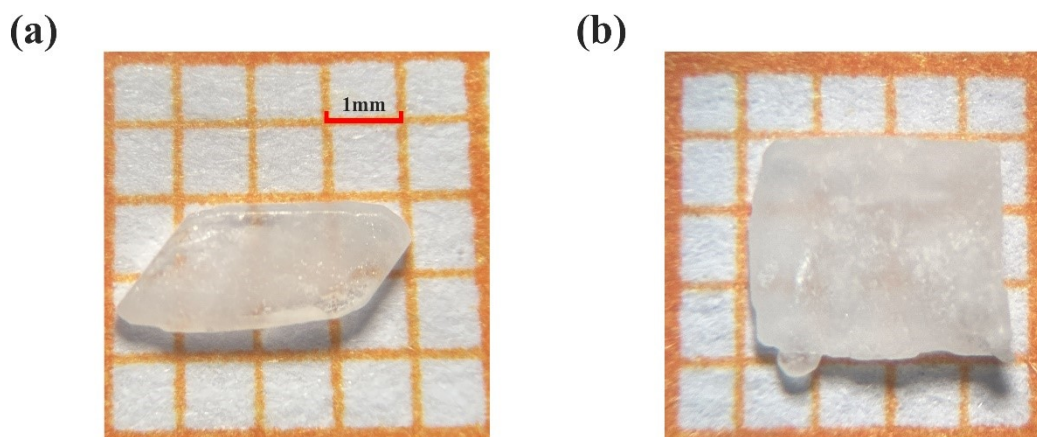


Fig. S1 The crystal photographs of (a) RbSbF₃Cl and (b) Rb₃Sb₄F₁₄Cl.

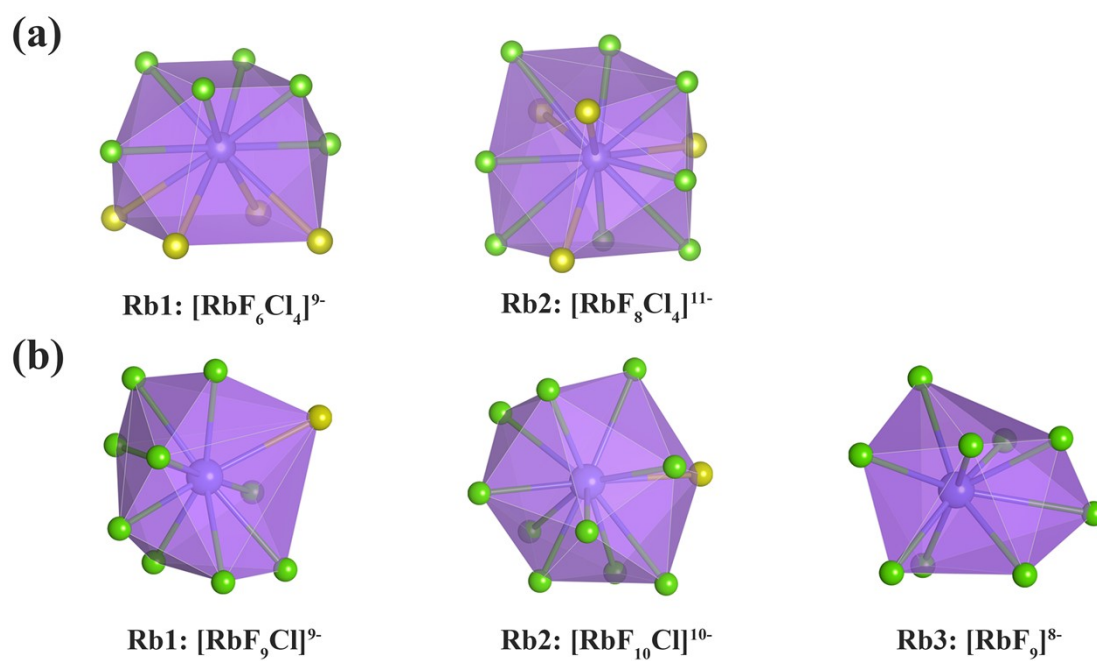


Fig. S2 The coordination modes of Rb⁺ cations in (a) RbSbF₃Cl and (b) Rb₃Sb₄F₁₄Cl.

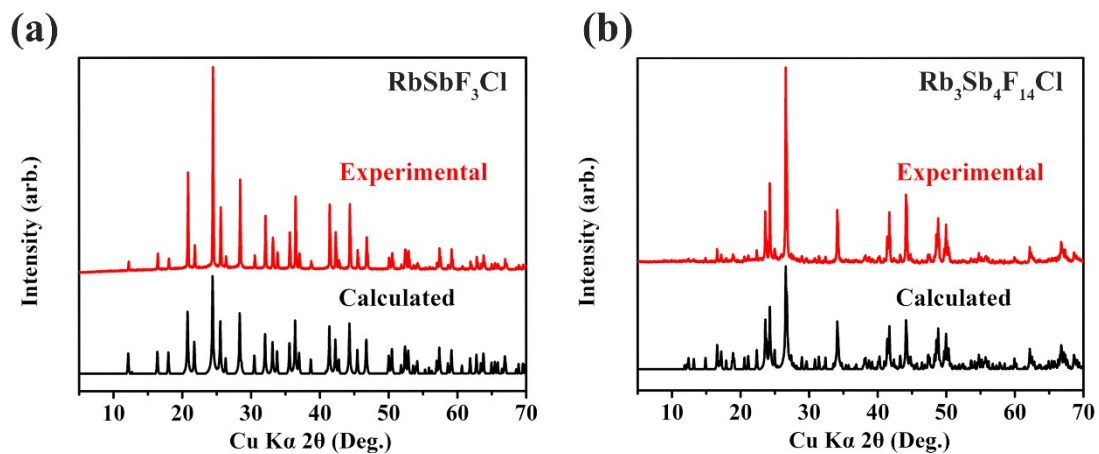


Fig. S3 Powder X-ray diffraction patterns of (a) RbSbF_3Cl and (b) $\text{Rb}_3\text{Sb}_4\text{F}_{14}\text{Cl}$.

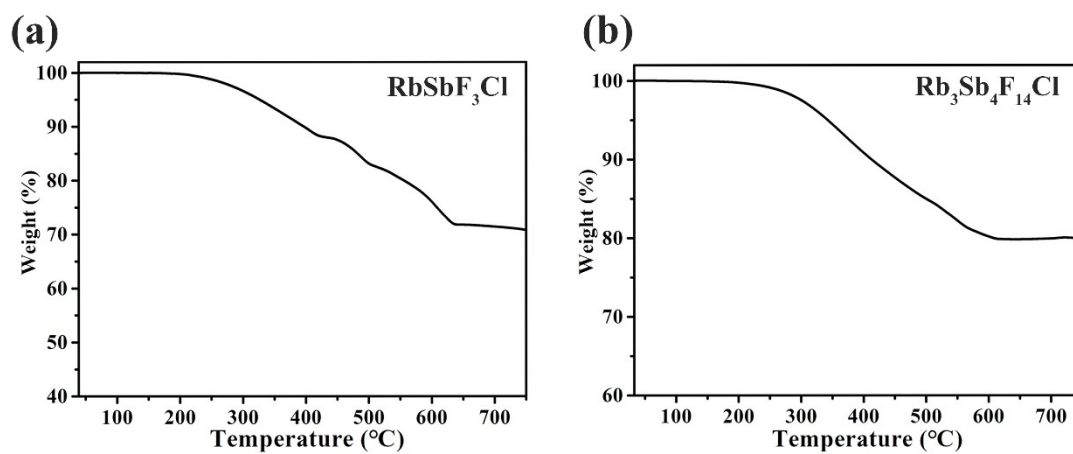


Fig. S4 TGA curves of (a) RbSbF_3Cl and (b) $\text{Rb}_3\text{Sb}_4\text{F}_{14}\text{Cl}$.

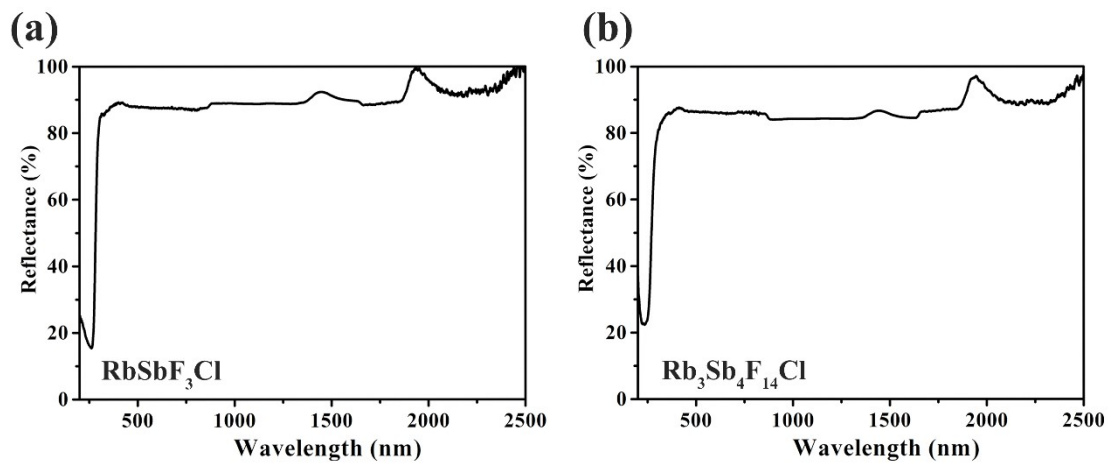


Fig. S5 UV-vis-NIR optical diffuse reflectance spectra of (a) RbSbF₃Cl and (b) Rb₃Sb₄F₁₄Cl.

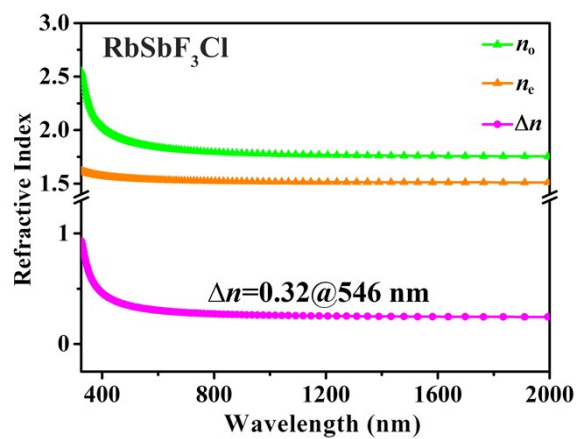


Fig. S6 Calculated refractive index for RbSbF₃Cl.

References

- (1) G. M. Sheldrick, A short history of SHELX, *Acta Crystallogr., Sect. A: Found. Crystallogr.*, 2008, **64**, 112–122.
- (2) A. L. Spek, Single-crystal structure validation with the program PLATON, *J. Appl. Crystallogr.*, 2003, **36**, 7–13.
- (3) S. K. Kurtz and T. T. Perry, A Powder Technique for the Evaluation of Nonlinear Optical Materials, *J. Appl. Phys.*, 1968, **39**, 3798–3813.
- (4) M. D. Segall, P. J. D. Lindan, M. J. Probert, C. J. Pickard, P. J. Hasnip, S. J. Clark and M. C. Payne, First-principles simulation: ideas, illustrations and the CASTEP code, *J. Phys. Condens. Matter*, 2002, **14**, 2717–2744.
- (5) D. Vanderbilt, Soft self-consistent pseudopotentials in a generalized eigenvalue formalism, *Phys. Rev. B.*, 1990, **41**, 7892–7895.
- (6) K. Kobayashi, Norm-conserving pseudopotential database (NCPS97), *Comput. Mater. Sci.*, 1999, **14**, 72–76.